

The orphan Sanriku tsunami of 1586: new evidence from coral dating on Kaua'i

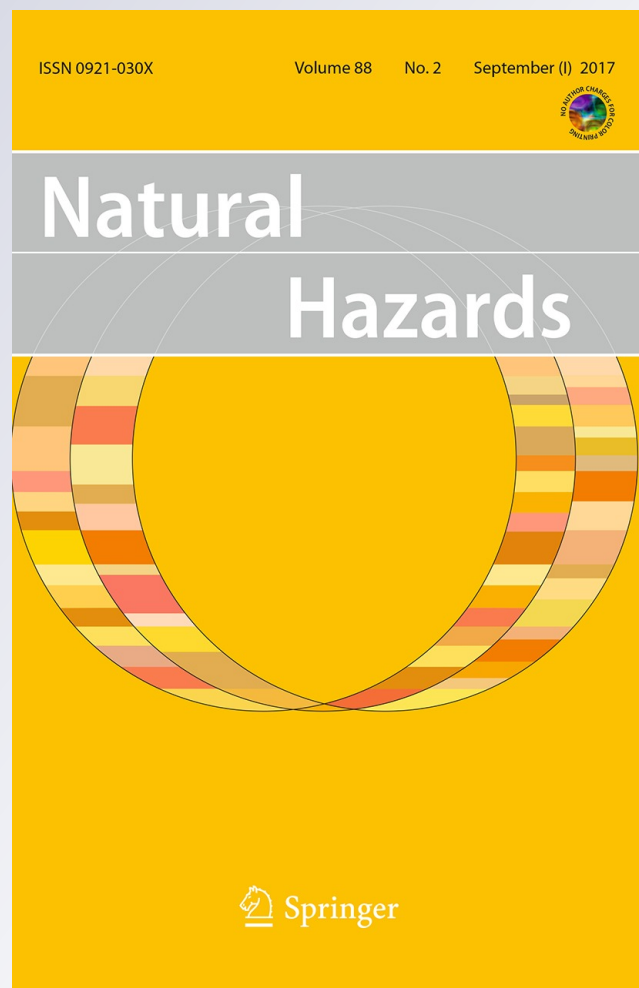
Rhett Butler, David A. Burney, Kenneth H. Rubin & David Walsh

Natural Hazards

Journal of the International Society
for the Prevention and Mitigation of
Natural Hazards

ISSN 0921-030X
Volume 88
Number 2

Nat Hazards (2017) 88:797-819
DOI 10.1007/s11069-017-2902-7



Your article is protected by copyright and all rights are held exclusively by Springer Science+Business Media Dordrecht (outside the USA). This e-offprint is for personal use only and shall not be self-archived in electronic repositories. If you wish to self-archive your article, please use the accepted manuscript version for posting on your own website. You may further deposit the accepted manuscript version in any repository, provided it is only made publicly available 12 months after official publication or later and provided acknowledgement is given to the original source of publication and a link is inserted to the published article on Springer's website. The link must be accompanied by the following text: "The final publication is available at link.springer.com".

The orphan Sanriku tsunami of 1586: new evidence from coral dating on Kaua'i

Rhett Butler¹  · David A. Burney² ·
Kenneth H. Rubin³ · David Walsh⁴

Received: 27 February 2017 / Accepted: 21 April 2017 / Published online: 4 May 2017
© Springer Science+Business Media Dordrecht (outside the USA) 2017

Abstract We have re-examined the historical evidence in the circum-Pacific for the origin of the 1586 orphan tsunami of Sanriku, Japan, previously attributed to a Lima, Peru, earthquake and tsunami in 1586. New evidence comes from corals found in a unique paleotsunami deposit on Kaua'i. Dated by ^{230}Th - ^{238}U geochronology these corals determine an absolute age in high precision of a Pacific tsunami event that was previously dated to approximately the sixteenth century by ^{14}C methodology. Detrital corrected ages of three low thorium, well-preserved coral clasts range from 415 to 464 years old (relative to 2016), with a mean age of 444 years ± 21 ($2\sigma_{\bar{x}}$). Literature evidence for circum-Pacific paleotsunami in this time range is reviewed in light of the new high-precision dating results. Modeled and observed tsunami wave amplitudes in Japan from several Peruvian events are insufficient to match the 1586 Sanriku observation, and paleodated earthquakes from Cascadia, the Alaskan Kodiak region, and Kamchatka are incompatible with the Sanriku data in several ways. However, a mega-earthquake ($M_w > 9.25$) in the Aleutians is consistent with the Kaua'i evidence, Pacific Northwest observations, and the Sanriku tsunami amplitude. The Kaua'i coral paleotsunami evidence therefore supports the origin of the 1586 Sanriku tsunami in the Aleutian Islands.

Keywords Orphan tsunami · 1586 Sanriku tsunami · Kauai Makauwahi corals · Tsunami modeling · ^{230}Th - ^{234}U - ^{238}U dating · Kauai, Aleutian Islands, Japan, Peru, Cascadia, South America

✉ Rhett Butler
rgb@hawaii.edu

¹ Hawai'i Institute of Geophysics and Planetology, University of Hawai'i at Mānoa, 1680 East-West Road, POST 602, Honolulu, HI 96822, USA

² National Tropical Botanical Garden, 3530 Papalina Road, Kalaheo, HI 96741, USA

³ Department of Geology and Geophysics, University of Hawai'i at Mānoa, 1680 East-West Road, POST 606, Honolulu, HI 96822, USA

⁴ Pacific Tsunami Warning Center, NOAA Inouye Regional Center, 1845 Wasp Boulevard, Building 176, Honolulu, HI 96816, USA

1 Introduction

Butler et al. (2014) studied a paleotsunami deposit on Kauaʻi discovered by Burney et al. (2001) in the Makauwahi Cave sinkhole (21.8883°N 159.4188°W) on the southeast coast (Fig. 1). The analysis of the probable run-up suggests its cause may be attributed to a mega-earthquake ($M_w > 9.2$) located in the Eastern Aleutian Islands (see Butler et al. 2017, for broader discussion of Aleutian earthquake sources). ^{14}C Carbon dating of short-lived plant material from the 80-cm-thick, paleotsunami layer indicates a severe marine event about four or five centuries ago (cal yr A.D. 1425–1660). The radiocarbon data are not able to provide an accurate high-resolution age because of vagaries in the ^{14}C production curve, atmospheric mixing of preformed carbon, and marine reservoir corrections over this time period. There is also legendary and archeological evidence since the arrival of the Hawaiian people (Butler et al. 2014). Herein we present ^{230}Th - ^{234}U - ^{238}U data from analysis of corals recovered from within the paleotsunami layer at the Makauwahi site and derive high-precision ages from them. Circum-Pacific paleotsunami evidence that may be contemporaneous with the Makauwahi coral dates is reviewed. Circumstantial and wave run-up model evidence suggests the Kauaʻi paleotsunami deposit may be connected to an “orphan” tsunami in Japan in 1586 (e.g., Atwater et al. 2005; Satake and Atwater 2007).

2 Makauwahi site

Makauwahi Cave, in the valley of Mahaʻulepu on the SE coast of Kauaʻi, is a karst feature in eolian calcarenite (Fig. 1). An unusual site within the largely volcanic Hawaiian Islands, it consists of cave passages with flowstone and dripstone formations, and a central collapse feature that is a sinkhole paleolake (Fig. 2). Clastic sediments on the sinkhole floor range to ca. 10 m thick, representing a nearly continuous record of Holocene events, include early Holocene marine incursion and subsequent roof collapse, brackish lake sedimentation throughout much of the Holocene, and nearly a millennium of human activity. Plant and animal fossils, and microfossils such as pollen and diatoms, are well preserved in the record.

Chronometric interpretations for the clastic deposits are supported by 40 published radiocarbon dates (Burney et al. 2001; Burney 2002; Burney and Kikuchi 2006). The paleotsunami deposit contrasts sharply with all other layers by its coarseness, including

Fig. 1 The *inset map* shows the location (red dot) of the Makauwahi sinkhole on the southeastern coast of Kauaʻi in the Hawaiian Islands. The scale for the *inset map* is about 12.2 km on a side. The town of Līhuʻe and Nawiliwili harbor is to the northeast. Figure from Butler et al. (2014), adapted with permission

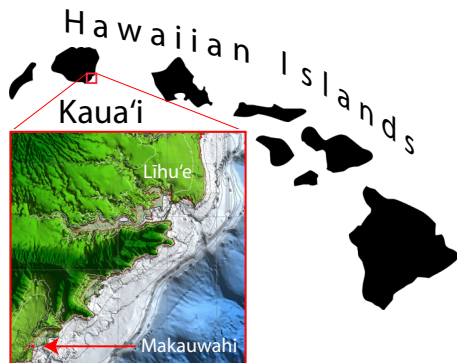




Fig. 2 The Makauwahi sinkhole, on the side of a lithified calcareous sand dune, is viewed toward the southeast from an apparent altitude of 342 m. *Inset photographs* show two of the wall edges, indicating the edges of the sinkhole. The east wall (*left*) is 7.2 m above mean sea level and about 100 m from the ocean. Note for scale the people in the right image. Photograph credits: RB (*left*), Gerard Fryer (*right*), GoogleMaps (background). Figure from Butler et al. (2014), adapted with permission

large fractured boulders, marine debris, and unsorted sand lenses, and is up to 80 cm thick in some places. To avoid issues of redeposition and inbuilt age, the inferred tsunami event is dated by four samples of relatively fragile, short-lived botanical materials in the deposit—three large exocarp fragments of kukui nut (*Aleurites moluccana*) and one gourd rind (*Lagenaria siceraria*), with a combined range at 2σ of 1425–1660 cal yr A.D.

The paleotsunami layer contains visually older reworked material that was mobilized from the underlying deposit by the high-energy deposition event. Although some redeposition is confirmed by unpublished ^{14}C dates cited in Liebherr and Porch (2015), the inferred radiocarbon age of the deposit is based upon the consilience of dates on short-lived botanical materials.

3 Corals

Natural coral skeletal fragments are common in the paleotsunami layer at Makauwahi Cave and rare in all other under and overlying units. Although some archeological materials in upper units of the site are made from coral, these are largely coralline files (Burney and Kikuchi 2006) made from modified fragments of dense corals of low porosity. Corals in the

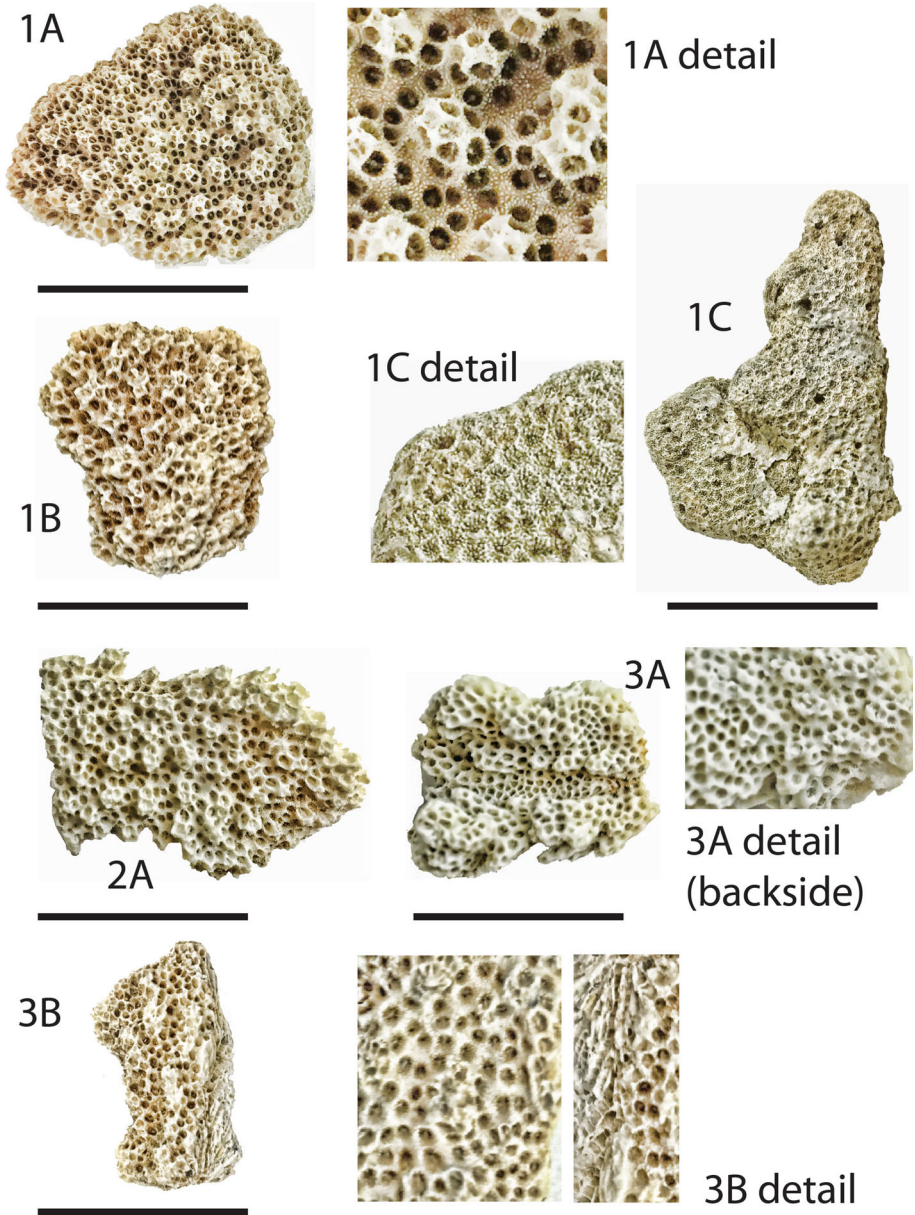


Fig. 3 Coral fragments analyzed in this study, labeled by bag number (1 through 3) and specimen identifier (A through C). Scale bars (2.54 cm) refer to whole specimen images (i.e., not the images labeled as “detail”). All pieces are small (3–5 cm in longest dimension). Specimens shown are after physical cleaning (in water). All specimens shown are corals of the genus *Pocillopora*, except 1C, which is *Porites*, and 3B, which is *Montipora*. These specimens were subsampled, chemically leached, and treated, and then small chips were selected under a microscope for U-series analysis

tsunami deposit, by contrast, include less dense and more porous types, such as cf. *Pocillopora* spp., that are in some cases relatively pristine, with no signs of human modification, mostly without heavy abrasion, and with minimal chemical alteration (e.g., Fig. 3). Samples were collected from depths of 2.6 to 3.0 m below datum in adjacent 1-m grid squares GG73 and GG74 of the excavated deposit and grouped into bags 1 through 5. All samples are thus from a 40-cm vertical interval, and no more than 2 m apart horizontally, in a deposit inferred from many lines of evidence (Burney et al. 2001) to have been laid down in a single high-energy event. About 20 of these coral fragments were examined visually for U-series dating potential. Dated samples were named for bag number and given fragment identifier (A, B, C).

The modern beach at Maha‘ulepu has many rocky patches and “microatoll” (algal mat) pockets in the tidal zone that frequently have dead coral fragments of unknown age. There are submarine limestone grottoes a few more meters below the tidal zone. Dead coral fragments from similar deposits could have been incorporated into the tsunami debris at the time of formation.

3.1 Description of specimens

Cleaned coral fragments displayed three characteristics (images of dated specimens are in Fig. 3) with respect to preservation of skeletal structures, infilling and coatings, and secondary colonization (coralgal overgrowth and/or shell casts or fragments, worm tubes, and borings). Specimens are divided into three general categories as indicated in Table 1: (1) morphologically pristine fragments with light but variable extents of meteoric alteration (coatings), which were likely living coral at the time of removal from the sea; (2) generally fresh but lightly colonized secondarily and with greater amounts of meteoric alteration (coatings and aragonite-to-calcite recrystallization), which likely had some post-death history within the source reef before deposition in the paleotsunami deposit; and (3) significantly altered or colonized fragments that likely have a significant post-coral-death seabed history. No type 3 fragments were analyzed in this study. Most of the well-preserved corals (especially in bags 2 and 3, but also bag 4) are *Pocillopora* sp. (likely, *P. meandrina*, a shallow water fingering coral). Rarer *Porites* and *Montipora* fragments are also present. All pieces were variably stained and occluded with clays and oxides. Bags 2 and 4 contained fragments with significant overgrowths and borings. The six visually freshest samples, three from category 1 and three from category 2, were selected for U-series dating (all non-dated coral clasts were less fresh).

3.2 Analysis methodology

Coral fragments from the paleotsunami deposit were examined for species, freshness, and type and style of coatings under a binocular microscope, both before and after initial physical and chemical pre-treatment to select the best candidates for ^{230}Th - ^{238}U dating. Initial cleaning was sequential washing in deionized water in a sonic bath until the water was clean, followed by organic matter removal with household bleach, and additional water washing in a sonic bath. Most fragments liberated significant iron-rich sediment during this process. All coral fragments retained some amount of discoloration after washing from iron-rich and organic deposits.

Samples were prepared and analyzed following methods described in Rubin et al. (2000) and Sherman et al. (2014). Samples were broken into small fragments (several mm in diameter) and pre-treated using the following sequence of solutions in a sonic bath:

Table 1 U-series geochronology and sample data ($\pm 2\sigma$)

| Analysis ID | IGSN | Coral preservation | Coral Genus | 238U (ppm) | \pm | 230Th (ppt) | \pm | 232Th (ppb) | \pm | (230Th/232Th) | \pm | |
|---------------|--------------|--------------------|---------------------------|------------|-------------|-------------|--------------|-------------|-------------------|---------------|----------|-------|
| Bag1 sample A | KHR30023C | 1 | <i>Pocillopora</i> | 2.790 | 0.009 | 0.225 | 0.024 | 1.319 | 0.002 | 31.9 | 3.4 | |
| Th rerun | | | | | | | | 1.357 | 0.003 | 29.4 | 3.4 | |
| Bag1 sample B | KHR30023D | 1 | <i>Pocillopora</i> | 2.935 | 0.008 | 0.251 | 0.024 | 1.844 | 0.003 | 25.4 | 2.4 | |
| Th rerun | | | | | | | | 1.900 | 0.007 | 27.4 | 2.7 | |
| Bag1 sample C | KHR30023E | 2 | <i>Porites</i> | 2.494 | 0.007 | 0.555 | 0.033 | 12.60 | 0.03 | 8.2 | 0.5 | |
| Th rerun | | | | | | | | 12.57 | 0.02 | 8.0 | 0.5 | |
| Bag2 sample A | KHR30023F | 2 | <i>Pocillopora</i> | 2.413 | 0.006 | 0.311 | 0.024 | 4.163 | 0.007 | 14.0 | 1.1 | |
| Th rerun | | | | | | | | 4.206 | 0.012 | 14.6 | 1.2 | |
| Bag3 sample A | KHR30023G | 1 | <i>Pocillopora</i> | 2.468 | 0.007 | 0.219 | 0.024 | 2.521 | 0.004 | 16.3 | 1.8 | |
| Th rerun | | | | | | | | 2.545 | 0.005 | 17.5 | 1.8 | |
| Bag3 sample B | KHR30023H | 2 | <i>Montipora</i> | 2.410 | 0.006 | 0.870 | 0.029 | 17.05 | 0.02 | 9.5 | 0.3 | |
| Th rerun | | | | | | | | 17.11 | 0.03 | 9.1 | 0.3 | |
| Analysis ID | (230Th/238U) | \pm | (230Th/238U) _d | \pm | (234U/238U) | \pm | Age (yrs bp) | \pm | Mean age (yrs bp) | \pm | Cal. age | \pm |
| Bag1 sample A | 0.0050 | 0.0005 | 0.0045 | 0.0006 | 1.142 | 0.005 | 432 | 50 | 413 | 39 | 1604 | 142.2 |
| Th rerun | 0.0046 | 0.0005 | 0.0047 | 0.0006 | 1.142 | 0.005 | 393 | 56 | | | | 142.2 |
| Bag1 sample B | 0.0053 | 0.0005 | 0.0047 | 0.0006 | 1.143 | 0.003 | 445 | 48 | 465 | 39 | 1552 | 143.4 |
| Th rerun | 0.0057 | 0.0006 | 0.0048 | 0.0007 | 1.143 | 0.003 | 484 | 49 | | | | 143.4 |
| Bag1 sample C | 0.0137 | 0.0008 | 0.0088 | 0.0009 | 1.144 | 0.003 | 845 | 79 | 827 | 37 | 1190 | 145.0 |
| Th rerun | 0.0133 | 0.0008 | 0.0089 | 0.0009 | 1.144 | 0.003 | 808 | 78 | | | | 145.0 |
| Bag2 sample A | 0.0080 | 0.0006 | 0.0063 | 0.0007 | 1.145 | 0.002 | 596 | 58 | 615 | 38 | 1401 | 145.8 |
| Th rerun | 0.0083 | 0.0007 | 0.0064 | 0.0008 | 1.145 | 0.002 | 634 | 59 | | | | 145.8 |
| Bag3 sample A | 0.0055 | 0.0006 | 0.0045 | 0.0007 | 1.141 | 0.003 | 429 | 56 | 450 | 41 | 1567 | 141.5 |

Table 1 continued

| Analysis ID | (²³⁰ Th/ ²³⁸ U) ± | (²³⁰ Th/ ²³⁸ U) _d ± | (²³⁴ U/ ²³⁸ U) ± | Age (yrs bp) ± | Mean age (yrs bp) ± | Cal. age ± | δ ²³⁴ U initial ± |
|---------------|--|---|---|----------------|---------------------|------------|------------------------------|
| Th rerun | 0.0059 | 0.0006 | 0.0007 | 1.141 | 0.003 | 52 | 141.5 |
| Bag3 sample B | 0.0222 | 0.0008 | 0.0009 | 1.143 | 0.002 | 73 | 144.3 |
| Th rerun | 0.0211 | 0.0008 | 0.0009 | 1.143 | 0.002 | 83 | 144.3 |

Parentheses indicate activity ratios; all uncertainties are given at the 2σ level and include decay constant uncertainties where appropriate

Coral preservation categories: (1) morphologically pristine; (2) light secondary colonization and meteoric alteration; (3) significantly altered or secondary biological colonization

Decay constants used: $\lambda_{234} = 2.8220 \times 10^{-6}$ and $\lambda_{230} = 9.1706 \times 10^{-6}$; $\lambda_{238} = 1.5513 \times 10^{-6}$; $\lambda_{232} = 4.948 \times 10^{-6}$

(²³⁰Th/²³⁸U)_d is the detrital corrected activity ratio. Calculated using two-point “osmond” isochron diagrams for secular equilibrium detritus using (²³²Th/²³⁸U) = 1.06 (i.e., average local rock, using mean Kilauea lava from Pietruszka et al. 2001); (²³⁰Th/²³⁸U) = 1, (²³⁴U/²³⁸U) = 1

Age and mean age in years before 2016 use detrital corrected (²³⁰Th/²³⁸U). Mean age is the average of both Th analyses per sample, which agree in all cases within stated uncertainties; calendar age = 2016 – mean age

δ²³⁴U initial is the decay corrected value, which should be within the range of modern sea water (142–147) for “reliable ages”

Additional sample bag notes

Bag 1. BAC-NW GG73 2.6 m 13/VII/2011 Several small pieces

Bag 2. BAC-NW GG73 2.8 m 18/VII/2011 Large piece and small fragments

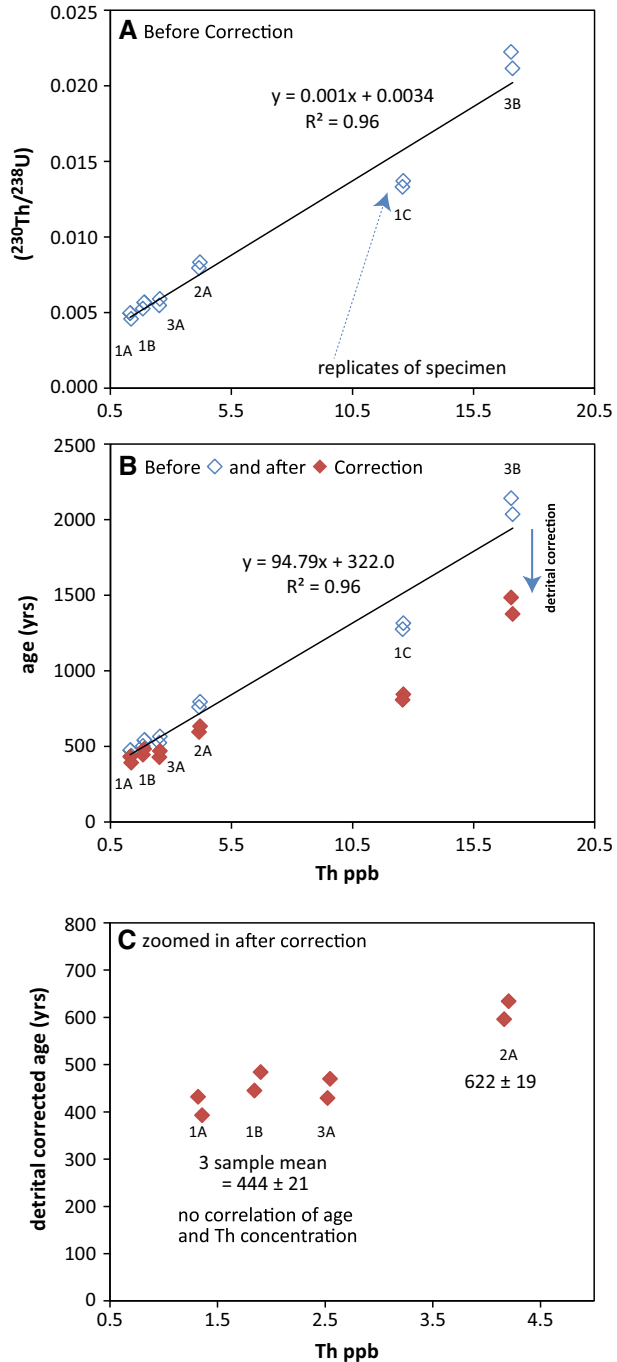
Bag 3. BAC-NW GG73 2.9 m 18/VII/2011 One medium and two small pieces

Bag 4. BAC-NW GG74 3.0 m 14 Jul 010 One medium and one small piece

Bag 5. BAC-NW GG73 3.0 m 19/VII/011 Two small pieces

“m” after a number represents meters below datum, the horizontal and vertical reference for excavation. The pit with the highest initial surface was at 0 m below datum, which is 1.82 m above present sea level. Therefore, these samples are from roughly 1 m below sea level, deposited in the brackish pond inside the sinkhole

Fig. 4 Effects of detrital correction on ($^{230}\text{Th}/^{238}\text{U}$) activity ratio and derived ages. U-series and age data are plotted for 2 replicate analyses on 6 different specimens (indicated with text labels 1A, 1B, etc.). The detrital correction method is described in Table 1 notes. (*upper panel*) Before correction ($^{230}\text{Th}/^{238}\text{U}$) is positively correlated with **Th** concentration, which is unlike living or “clean” skeletal fossil coral (i.e., defined as those with less than 2 ppb **Th**). (*middle panel*) Ages are correlated with **Th** before detrital correction. The entire group remains correlated with **Th** concentration after correction, albeit at lower slope. (*lower panel*) Ages of the three lowest **Th** (and youngest specimens) are not correlated with **Th** concentration, indicating that the detrital correction is robust for these samples



H₂O₂/NaOH solution (for organic matter digestion), ultrapure water (quartz subboiling distilled Milli-Q feedstock), 0.05 M HNO₃ solution (5-min wash for adsorbed **Th** and **U** removal), and double washing in ultrapure water. Samples were dried under filtered air,

Table 2 Paleotsunami and historical sites discussed in text and shown in Figs. 5 and 6

| Index to Fig. 5 | Site | ¹⁴ C calibrated years A.D. ^a | References |
|-----------------|--|--|--|
| T2 | T2 turbidite flows Oregon–Washington | 1402–1502 ±2σ | Goldfinger et al. (2012) |
| 1 | Deserted Lake, N Vancouver Island, B.C. | 1380–1590 ±σ | Hutchinson et al. (2000), Peters et al. (2007) |
| 2 | Discovery Bay, WA | 1450–1650 ±σ | Williams et al. (2005) |
| 3 | Grayland Plains, WA | 1400–1630 n/a | Schlichting (2000), Schlichting et al. (1999), Peters et al. (2007) |
| 4 | Youngs Bay, Columbia River, OR | 1425–1650 n/a | Peterson et al. (1993), Peters et al. (2007) |
| 5 | Ecola Creek, OR | 1500–1740 ±σ | Peterson et al. (1993), Darienzo and Peterson (1995), Peters et al. (2007) |
| 6 | Netarts, OR | 1545 to 1635 ±2σ | Shennan et al. (1998) |
| 7 | Alsea Bay, OR | 1120–1675 ±σ | Darienzo (1991), Darienzo and Peterson (1995), Peterson and Darienzo (1996), Peters et al. (2007) |
| 8 | Lily Lake, OR | 1220–1700 n/a | Briggs and Peterson (1992), Peters et al. (2007) |
| 9 | Kronotskiy Bay, Kamchatka, Russia | 1500–1670 ±σ | Pinegina et al. (2003), Pinegina and Bourgeois (2001) |
| 10 | Makauwahi Cave, Kaua'i, HI | 1425–1660 ±σ 1551–1593 ±2σ | Burney et al. (2001) This study |
| 11 | Sedanka Island, AK | 1527–1664 ±σ 1650–1780 ±σ | Witter et al. (2015) |
| 12 | Kodiak-Katmai, AK | 1440–1620 ±2σ | Shennan et al. (2014a, b) |
| 13 | Aitutaki, Cook Islands | ca. sixteenth century | Allen and Wallace (2007), Goff et al. (2011) |
| 14 | Rurutu, Austral Islands | 1450–1600 | Bollt (2008), Goff et al. (2011) |
| 15 | Suijin-numa, Sendai Coast, Japan | 1440–1600 ±2σ | Sawai et al. (2008) |
| 16 | Miyagi Prefecture, Sanriku, Japan | Sept. 1586 (historical record) | Hay (1605), Mallet and Mallet (1858), Heck (1947), Solov'ev and Go (1975), Iida (1984), Tsuji (2013) |

n/a not available

^a Error bounds as published in openly available references

and the most pristine fragments were selected for analysis under a microscope. Those fragments were weighed (masses are in Table 1), dissolved in HNO₃, inspected for undigested detrital silicate material by centrifugation (none observed), spiked with calibrated ²²⁹Th and ²³³U tracers, and dried/redissolved in 8 M HNO₃ to equilibrate. Th and U were separated and purified using anion exchange chemistry and analyzed by thermal

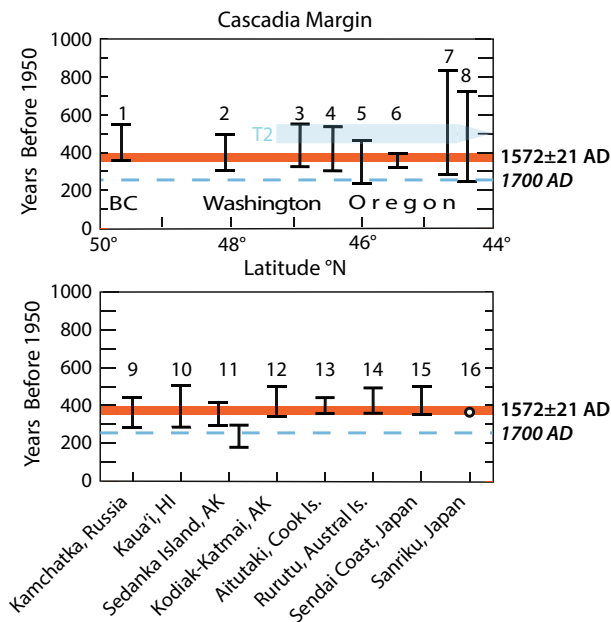


Fig. 5 Circum-Pacific paleotsunami and historical evidence contemporaneous with Kaua‘i mean coral date (1572 A.D.) shown in orange (line width is $2\sigma_{\bar{x}}$ uncertainty). Dashed blue line shows the year of the 1700 Cascadia event (Atwater et al. 2005). Light blue line (T2) in upper figure shows 2σ uncertainty of a dated turbidite flow prior to 1700 event. Data sources are in Table 2, and numbered locations are shown in Fig. 6. Note that in the upper figure the sites in the Pacific Northwest—British Columbia (BC), Washington (WA), Oregon (OR)—are ordered by latitude from north to south, whereas the lower figure encompasses other Pacific Island and coastal sites. The two date estimates for Sedanka Island, Alaska, reflect both a single sample that overlaps the uncertainty of the coral dates, and a Bayesian estimate that does not, respectively

ionization mass spectrometry. Resulting data are presented with and without standard 2-point detrital Th corrections (see Table 1 notes for details and the discussion section).

3.3 Unique characteristics

Two characteristics of this sample set are atypical for most ^{230}Th - ^{238}U fossil coral dating studies and bear on the interpretation of the ages: the very young ages and the relatively high-Th concentrations (up to 17 ppb). ^{230}Th - ^{238}U dating at this young age is made difficult by the small amount of radiogenic ^{230}Th ingrowth (half-life is 75.6 kyr), uncertainties about ^{230}Th concentrations in living corals, and potential “detrital” Th addition after specimen death (e.g., Edwards et al. 1988; Zachariassen et al. 1999; Cobb et al. 2003). Extremely small ^{230}Th concentrations (as well as small amounts of unaltered sample available for analysis) made mass spectrometric analyses of these specimens difficult, resulting in higher relative error than is typical for ^{230}Th - ^{238}U dating of older corals. For this reason, Th in each sample was analyzed in duplicate and found to agree within analytical uncertainty in each case (see Table 1). Detrital Th corrections (e.g., see review in Edwards et al. 2003) were made for each sample using average Hawaii volcanic rock

compositions (as described in Table 1 notes). These corrections affect ages by 50–60 and 475–665 years for low-**Th** and high-**Th** samples, as discussed below.

3.4 ^{230}Th - ^{238}U analysis results

Coral ages and uncertainties in Table 1 were calculated by standard methods. Although many publications in the literature present only detrital corrected ages, we present ages calculated with and without detrital corrections so readers can assess the magnitude of the shift. Corals of this study can be divided into two categories by **Th** concentration. (a) Low-**Th** specimens (samples 1A, 1B, 3A) required minimal detrital **Th** correction, and ages agree better between them after correction; (b) variably higher **Th** concentration specimens (2A, 2B, 3B) required larger detrital correction and show wider spread in apparent ages. Apparent ages in group (b) correlate with **Th** concentration, both before and after detrital correction (see Fig. 4), indicating that the high-**Th** samples picked up significant ^{232}Th and ^{230}Th from the environment. This is despite the fact that only non-**Fe**-stained subsamples and those lacking visible microscopic detritus within the skeleton were analyzed, as confirmed by complete acid dissolution of each specimen and lack of silicate residue after dissolution.

Detrital corrected ages of the 3 low-**Th** samples (each of the 3 sample duplicates were averaged, weighted by their variance) range from 415 to 464 years old (relative to 2016), with a mean age of 444 years ± 21 ($2\sigma_{\bar{x}}$), which is a smaller range than the roughly 50-year analytical uncertainty (including half-life uncertainty) of individual specimen ages. Detrital correction removes all aberrant relationship of age and **Th** concentration that exists in the uncorrected data in this sample group, lending confidence to the method and absolute amount of correction (i.e., more or less correction would leave a residual correlation). These ages expressed in calendar years have a mean at the year 1572 ± 21 ($2\sigma_{\bar{x}}$). We interpret this date as both the age of the deposit and the time of coral death (when they were removed from the ocean and deposited) because of the visually pristine nature of these skeletons and the nearly identical ages of the three specimens within uncertainty. Although it is possible that the tsunami layer in the cave deposit could post-date the age of these corals, it is difficult to model a deposition timescale from the thin, poorly sorted deposit itself. In any event a significant (relative to the radiometric precision) time span in between coral death and deposit incorporation is inconsistent with the visual observations of these clasts. Finally, if the youngest corals sampled were indeed already dead prior to the tsunami, then the corals pre-date the tsunami, implying a more recent date for the tsunami. However, the tsunami is still constrained by the ^{14}C dates as < 1660 cal yr A.D. References to coral residence time on a reef and carbonate fragment transport through the littoral zone have only mild relevance here (e.g., Ford and Kench 2012; Ford 2014) because the settings differ, and further field surveys to constrain the local residence times are beyond the scope of the present investigation.

The specimens with higher **Th** concentration have older apparent ages (at 615 ± 38 ; 827 ± 37 ; 1430 ± 108 (all $2\sigma_{\bar{x}}$) years before present, equivalent to calendar ages of 1401, 1190, 586). Although ages are calculated for these higher **Th** corals, they do not record time since coral death. These apparent ages are 173, 384, and 988 years older than the mean age of the low-**Th** group of 444 years. All of these ages are well within the range of coral ages in modern Hawaiian reef structures (Easton and Olson 1976) but these high-**Th** coral results do not record actual coral age within the reef at the time of removal from the ocean. Because of the strong correlation of apparent age with ^{232}Th concentration, we believe this reflects unaccounted for detrital ^{230}Th from a source that is isotopically

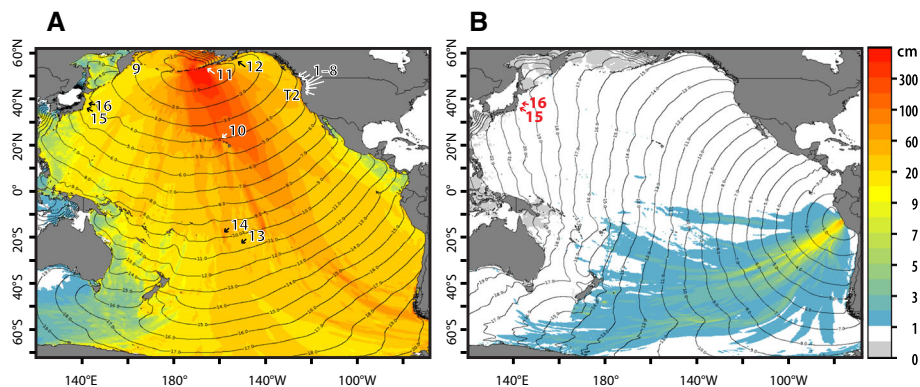


Fig. 6 **a** Locations of paleotsunami deposits and historical records contemporaneous with Kaua'i (site 10) results. Numbered locations are referenced to Table 2. Background is an illustration of forecast open-ocean tsunami amplitudes (scale in cm shown at right) for a M_w 9.25 earthquake in the Eastern Aleutian Islands modeled in Butler et al. 2014 (600 km \times 100 km in area and 35-m fault displacement). **b** Tsunami forecast for a M_w 8.05 earthquake located at the site of a 1586 earthquake near Lima, Peru. NB the tsunami amplitude of the Eastern Aleutian event along the Sanriku coast of Japan (site 16) better matches reported observations (Solov'ev and Go 1975) than a modeled, 1586 earthquake consistent with historical seismic intensities reported in Peru

different than local volcanic rock. We do not believe that open-system recoil addition of ^{230}Th (e.g., Thompson et al. 2003) after emplacement in the deposit has occurred because all dated corals have initial $^{234}\text{U}/^{238}\text{U}$ (expressed as $\delta 234$) within the range of modern seawater. In summary, the lack of cementation, biological overgrowths, biological borings, and age versus ^{232}Th in the low- Th samples indicate that these are the most reliable actual ages. The higher Th corals, although still relatively low in overgrowths, cementation, and borings, have been compromised by post-death Th addition.

4 Review of contemporaneous paleodata in the Pacific

The precision of the low- Th coral dates is sufficient to provide for practical comparison with historical evidence in Japan and South America. We also review available contemporaneous Pacific paleotsunami data including: the Aleutian Islands; the Alaskan Peninsula, Kodiak Island, and Prince William Sound subduction margin; the Cascadia margin of North America; South Pacific Islands; and Kamchatka. Figure 5 and Table 2 present the dated intervals discussed herein. Figure 6 shows the paleodata sites, and a historical site in Japan, in the context of a Pacific-wide tsunami originating in the Eastern Aleutian Islands. Additionally, Butler et al. (2016) discuss median recurrence rates for $M_w \geq 9.0$ earthquakes compared with regional paleotsunami observations.

4.1 Japan and South America

In discussing the orphan tsunami of 1700 in Japan from Cascadia, Atwater et al. (2005) mention “foreign waves” from an “orphan tsunami” observed in 1586 “known in Japan only from the southern Sanriku coast only.” Satake and Atwater (2007) reiterate, “... orphan tsunamis have been linked securely to earthquakes and tsunamis in South America,

beginning in 1586...”. We review the evidence for this earlier event, which is within the range of our coral dates for Kaua’i.

Japan experienced a tsunami along the southern Sanriku coast in 1586 (possibly 1585, see below) that was not correlated with a local earthquake (Tsuji 2013): “A legend in Tokura village in Minami Sanriku town, Motoyoshi County, Miyagi Prefecture says that a tsunami came to the coast of the village in the 14th year of the Tensho Period,” which is 1586. “According to an inscription on a monument in Tokura (the prefecture of Miyagi), a tsunami arrived at the northeast shore of the island of Honshu, where it reached a height of 1–2 m” (Solov’ev and Go 1975; referencing Acosta; 1621; Parish 1836, 1838; von Hoff 1840; Mallet 1855; Ponyavin 1965; Iida et al. 1967).

K. Satake (personal communication, 2017) added, “Apparently [the information] was collected after the 1896 Sanriku tsunami, and the date of the tsunami was originally 14th day of 5th month of Tensho 13th year (June 1 in 1585 on Julian calendar or June 11 on Gregorian calendar). How accurate [is] this date in legend is not known, but a few reports published after the 1933 tsunami mentioned this date. Then after the 1960 Chilean tsunami, Ninomiya (1960) compiled historical tsunami data and apparently correlated it with the 1586 Peruvian earthquake, even though the dates are different. Ninomiya did not ‘securely’ correlate[] these two. The oral legend mentioned about tsunami only, hence it can be considered as ‘orphan’ tsunami, but the possibility of local earthquake cannot be ruled out.”

The National Centers for Environmental Information mentions both the 1585 and 1586 tsunamis in Sanriku, noting in references that the two events may be the same event with mistaken attribution. There is a separate, third tsunami associated with an earthquake at Ise Bay near Osaka on January 18, 1586. For the sake of consistency, the two aforementioned 1585/1586 events will be termed “1586,” as this date is already attributed in several papers.

Sawai et al. (2008) found paleotsunami evidence of a marine incursion dated 1440–1600 A.D. (95% confidence interval) from the Sendai coast at Suijin-numa, a coastal lake facing the Japan Trench. Although stating the evidence is “most probably deposited by the 1611 Keicho tsunami, though deposition by the 1648 storm surge cannot be entirely ruled out,” there is no discussion of the 1586 orphan tsunami in this context even though it is adjacent to the Sanriku coast and actually matches the dated time interval. Nonetheless, the paleotsunami evidence is corroborative of the historical tsunami accounts from Sanriku.

The 1586 event fits the timing of the Kaua’i coral dates within their precision (Fig. 5). Modeling the tsunami coastal estimates along the Sanriku coast of Japan using the NOAA SIFT code (e.g., Gica et al. 2008) model for the M_w 9.25 Eastern Aleutian event (Butler et al. 2014), the tsunami coastal forecasts at Ōfunato and Hachinohe along the Sanriku coast are 104 cm and 83 cm, respectively, and compare reasonably well with the historical account (Fig. 6a), given factor of two (or more) uncertainty in coastal estimates where precise locations cannot be obtained. This basic Eastern Aleutian source model—a fault with dimensions 600×100 km² with 35 m of slip—has not been adjusted for possible variations in fault rupture, rupture velocity, and fault extent, each of which can amplify the tsunami further. Forecast models including rupture into the 1957 earthquake zone (e.g., Butler et al. 2017) have shown tsunami amplitudes exceeding 1.5 m along the Sanriku coast. Slow, unilateral rupture of the earthquake fault from east to west, and enhanced slip to the west, will further enhance tsunami energy directed west toward Japan.

We have utilized the SIFT model for several reasons. The SIFT code is a US national standard tsunami code, validated and tested, and used to safeguard the lives of millions of coastal people. The SIFT code computes “coastal estimates” for 320 sites around the circum-Pacific. These estimates, and those from the Pacific Tsunami Warning Center

linearized “RIFT” code, are used to derive tsunami coastal warnings throughout the Pacific. For sites discussed in the USA, we employ the full SIFT Stand-by Inundation Models (SIFT/SIM) to forecast the coastal inundations. As detailed bathymetry and coastal DEMs are not generally available outside of the USA—in particular, from the Japanese Sanriku coast—the only recourse is to use coastal estimates that are readily available from realistic propagation models, such as SIFT. Obviously, there are no DEMs of the actual shoreline in the sixteenth century. Nonetheless, better estimates may possibly be obtained in the future through collaboration with Japanese tsunami modelers.

The 1586 tsunami in Sanriku has recently (Ninomiya 1960; Solov’ev and Go 1975; Iida 1984) been attributed to a large earthquake 15,000 km distant in Peru on July 9. Okal et al. (2006) have examined this hypothesis and noted inconsistencies. Flooding is mentioned only at one site near Lima and not elsewhere in Peru. A macroseismic investigation throughout Peru of the reported historical earthquake intensities in 1586 indicates a relatively short earthquake rupture length of only 175 km (Dorbath et al. (1990), comparable in the size, location, and intensity to the Peruvian earthquakes of 1974 (M_w 8.1) and 2007 (M_w 8.0) (Tavera and Bernal 2008). Both of these events produced a small tsunami in Japan averaging 7 and 4 cm, respectively, along the Sanriku coast (NCEI 2017). Further, prior mega-earthquakes in Peru in 1687 and 1868 estimated at M_w 8.9 and 9.2 (Okal et al. 2006) have much more substantial observed run-ups of 0.5–2 m and 1–3 m in Japan, respectively (NCEI 2017).

To view the tsunami forecast and impact upon the Sanriku coast of Japan, we modeled M_w 8.05 earthquakes at the Peruvian subduction zone using the SIFT tsunami code ($200 \times 50 \text{ km}^2$ fault area and 3.5 m slip, both near to the trench and coastward). The results are shown in Fig. 6b where open-ocean amplitudes are less than a few centimeters. Coastal amplitudes in Japan are forecast at 6 ± 3 (1σ) cm, matching the observed tide gauge amplitudes of the 1974 and 2007 Peruvian events in Japan.

We may summarize the evidence discounting the Peruvian origin for the 1586 Sanriku orphan tsunami: (1) the reported earthquake intensities for the 1586 earthquake in Peru are not consistent with the extended fault rupture characteristic of a great ($M_w > 8.5$) earthquake (Dorbath et al. 1990); (2) the observed pattern of earthquake intensities for the M_w 8 Peruvian earthquakes in 1974 and 2007 is comparable to those for the proximal 1586 event (Dorbath et al. 1990; Tavera and Bernal 2008); (3) observed tsunami amplitudes on the Sanriku coast from the 1974 and 2007 Peruvian earthquakes average < 10 cm (NCEI 2017); and (4) tsunami modeling of the 1586 Lima, Peru, earthquake forecasts tsunami amplitudes on the Sanriku coast of 6 cm (Fig. 6b). Therefore, based upon observed earthquake intensities in Peru and tsunami amplitudes in Sanriku from comparable Peruvian earthquakes in 1974 and 2007, as well as the forecast tsunami amplitudes in Sanriku, the Peruvian origin for the Sanriku orphan tsunami of 1586 may be discounted.

The closest historical, great earthquake in Peru occurred in 1604 (M_w 8.7, Dorbath et al. 1990). Elsewhere on the western South America margin, there is no mention of a 1586 earthquake. In Ecuador, the 1587 Guayllabamba earthquake is estimated at $M_w < 7$ based upon isoseismal intensities surrounding Quito (Beauval et al. 2010) and produced a tsunami: “The sea left its bed, generating a giant wave which is believed to have destroyed the village of Sechura, in northernmost Peru, which was relocated on the site it now occupies” (Silgado 1973). In northern and central Chile, there is no contemporaneous, great earthquake (Dura et al. 2015). Lomnitz (1970) discusses the 1575 Valdivia earthquake (M_w 8.5; Askew and Algermissen 1985) in southern Chile, which deposited coastal paleotsunami evidence over the northern half of the great 1960 Chilean earthquake fault rupture zone

(Cisternas et al. 2005; St. Onge et al. 2012; Moernaut et al. 2014). However, none of these events produced a measured tsunami in Japan (NCEI 2017).

In reviewing the observability of an orphan tsunami, local tide levels must be considered. In South America (Ecuador, Peru, Chile) the maximum tidal variation ranges from 1 to 4 m, with mean variation at about 60% of the maxima. Along the Sanriku coast, the maximum tidal variations are about 1.4 m. These tidal variations are comparable to the forecast tsunami coastal estimates, as well as the observed tsunami in 1586 in Sanriku. Hence, there is a stochastic quality about whether distant tsunamis may or may not be observed, whether in Japan or South America.

The correspondence of the date 1586 for the Peruvian earthquake, the Sanriku tsunami observed in Japan, and the precision of the coral dates from Kaua'i bears further examination. Reviewing the literature, the earliest western source mentioning the Sanriku tsunami appears to be *De Rebus Japonicis, Indicis & Peruanis Epistolae Recentiores* (Hay 1605). This contains a collection of letters and reports (in Latin) edited by John Hay, a Jesuit priest, who is referenced in the *History of Japan* (Kämpfer 1727). Subsequently referencing the foregoing, the Earthquake Catalogue of the British Association (Mallet and Mallet 1858) refers separately to the Lima, Peru, earthquake of July 9, 1586, and the Sanriku tsunami of September 1586. More recently, Heck (1947) followed Mallet and Mallet (1858) and listed the 1586 Peruvian event as separate from the Sanriku tsunami. The conjunction of these as the same event appears in Solov'ev and Go (1975) and Iida (1984), but without any apparent reference to the Japanese source (Ninomiya 1960) connecting the mutual dating.

4.2 Kamchatka

Tatiana Pinegina and colleagues have extensively mapped paleotsunami deposits on the eastern coast of Kamchatka (Pinegina et al. 2000; Pinegina and Bourgeois 2001; and Pinegina et al. 2003). Tsunami events are noted in Kronotskiy, Avachinsky, Asacha, and Mutnaya Bays nominally dated 1500, 1550, and 1600 A.D. (Pinegina and Bourgeois 2001). Assuming uniform peat deposition between Holocene dated tephras, Pinegina et al. (2003) find tsunami layers at 1580–1590 and 1570–1590 A.D. near the mouth of the Zhupanova River, southern Kronotskiy Bay. Uncertainties in the dating of a key tephra layer are stated as ± 87 years. Tsunami forecast coastal estimates at Ust and Petropavlovsk are 146–155 cm, based upon the Aleutian earthquake source model of Butler et al. (2014). Conversely, the observed tsunami run-ups in Sanriku (Miyagi and Iwate prefectures) from the M_w 9 Kamchatka earthquake of 1952 average at 189 ± 72 cm. Hence, Kamchatka holds evidence on the 1586 orphan tsunami of Sanriku, whether as a possible source (assuming an event comparable to 1952) or as an inundation site from an Aleutian earthquake.

We note above the lack of paleotsunami evidence along the western margin of South America. Using the same earthquake source used for modeling the Kaua'i paleotsunami deposit (Butler et al. 2014), tsunami coastal estimates in Sanriku range from 83 to 104 cm. For the South American margin, the coastal estimates average at 152 ± 61 cm. However, for perspective let us compare another pair of events: the Kamchatka earthquakes of 1952 and 1737. The 1952 (M_w 9.0) earthquake generated a tsunami along the Chilean coast of 90–143 cm. The October 1737 event is considered to be as large or larger than the 1952 earthquake (Pinegina and Bourgeois 2001). Run-ups of > 50 m (Krashennikov 1755) were reported along the Kamchatka coast exceeding the maximum 39-m run-up (Mori et al. 2011) from 2011 Tohoku observed in Japan. The tsunami run-up on Amchitka Island was evidenced by large quantities of driftwood, piled forty and fifty feet (15 m) above high

water, that were attributed by local inhabitants to the 1737 earthquake. However, the 1952 event has measurements on Attu and Adak, which bound Amchitka, of 1.9 and 1.1 m, respectively—indicating that in the nearby Aleutians, the 1737 tsunami was the larger, but likely had a different distribution of faulting. However, there are no historical accounts in Chile of a tsunami from this October 1737 Kamchatka event. Furthermore, the local historical accounts of a large earthquake ($M \sim 8$; Askew and Algermissen 1985) in December 1737 in southern Chile specifically indicate no tsunami in any account from Concepción, Valdivia, and Isla Chiloé (Lomnitz 1970; Cisternas et al. 2005). Therefore, the lack of evidence of an “orphan tsunami” from the Aleutians in 1586 is no more substantial than the lack of tsunami evidence from the great Kamchatka earthquake of 1737 in Chile.

4.3 Aleutian Islands

A single paleotsunami site at Stardust Bay on Sedanka Island in the easternmost Aleutians has six dated tsunami events in the past 1600 years (Witter et al. 2015). The most recent deposit corresponds to the M_w 8.6 1957 earthquake in the central Aleutians. Using a Bayesian algorithm (Bronk-Ramsey 2009) and a pair of discordant ^{14}C dates, Witter et al. (2015) estimated the age of the paleotsunami layer immediately underlying the 1957 layer at 300–170 cal yr BP (1650–1780 A.D.), which post-dates the Kaua‘i deposit. Nonetheless, one ^{14}C -dated sample of two found beneath the base of the penultimate tsunami layer of the Sedanka site was observed to have a date contemporaneous with the Makauwahi corals: cal yr 1527–1664 A.D., the other is more recent than 1666 A.D. but otherwise unconstrained. A SIFT/SIM tsunami forecast run-up at Unalaska, AK, is 260 cm, based upon the Aleutian earthquake source model of Butler et al. (2014). Since Sedanka Island faces the Pacific and the town of Unalaska faces the Bering Sea, the tsunami forecast is a minimum.

4.4 Alaska

Preceding the great 1964 Alaskan earthquake (M_w 9.2), history records a double event on July 21 and August 8, 1788 A.D. (Hatori 2005; Shennan et al. 2014a), likely rupturing the subduction zone at Kodiak Island. No tsunami was mentioned in Japan (Iida 1984; NCEI 2017). There is ample paleoseismic and archeological evidence in southern Alaska pre-dating the 1788 earthquake informing the tsunamigenic history of the region (e.g., Carver and Plafker 2008; Combellick 1991, 1993, 1994; Combellick and Reger 1994; Shennan et al. 2009, 2014a, b; Hamilton and Shennan 2005a, b; Hutchinson and Crowell 2006, 2007; Gilpin 1995). In the region of Prince William Sound, the Kenai Peninsula, and the Copper River delta on the eastern coast, there are no great earthquakes between 1964 and 1089 ± 53 (2σ) A.D. At Kodiak Island, there is an evident paleotsunami (Gilpin 1995; Carver and Plafker 2008) that has been reinterpreted (Shennan et al. 2014a) with additional data as 1440–1620 A.D. (2σ bounds). Archeological evidence on Kodiak and Katmai coastal sites (abandonment or tsunami incursion) suggests a paleotsunami at 1350–1600 A. D. (most likely minimal and maximal ages). A SIFT/SIM tsunami forecast run-up at Kodiak, AK, is 105 cm, based upon the Aleutian earthquake source model of Butler et al. (2014).

Nonetheless, considering Kodiak to have been the source of the 1586 tsunami, the challenge is the limited size of faulting as constrained by other regional paleotsunami observations, and the fact that the geometry of the Kodiak margin directs tsunami energy toward the southern tip of South America. Furthermore, even the M_w 9.2 Alaska

earthquake of 1964—which includes rupture of the Kodiak Island segment—generated a tsunami in Sanriku of only 38 ± 26 cm.

4.5 Cascadia

The Cascadia coast of North America is the site of a major tsunami in 1700 which is observed in paleotsunami evidence along the Cascadia margin (e.g., Peters et al. 2007), as well as in historical accounts of an “orphan” tsunami observed in Japan (i.e., without a local earthquake source, Atwater et al. 2005). Nonetheless, an examination of the paleotsunami studies (Briggs and Peterson 1992; Darienzo 1991; Darienzo and Peterson 1995; Hutchinson et al. 2000; Peterson and Darienzo 1996; Peters et al. 2007; Peterson et al. 1993; Schlichting 2000; Schlichting et al. 1999; Shennan et al. (1998); Williams et al. 2005) shows distinct evidence for a tsunami prior to the 1700 Cascadia event at eight sites (Fig. 5) from British Columbia to Oregon, as well as a range of sites with dates overlapping the 1700 event (Peters et al. 2007). Goldfinger et al. 2012 have analyzed off-shore turbidites along the Cascadia margin, deriving more than 18 paleoevents dating back 10,000 years. The most recent event (T1) corresponds to the 1700 AD event, and a prior, smaller event (T2) is dated at 1402–1502 A.D. ($\pm 2\sigma$ range).

The precision of the turbidite dates for event T2 effectively removes Cascadia from consideration as the source region for the 1586 orphan tsunami in Sanriku. However, the dated paleotsunami events along the Cascadia margin of British Columbia, Washington, and Oregon—particularly the Netarts Bay deposits (Shennan et al. 1998)—are consistent with an Aleutian origin. Furthermore, as a proxy for a Kamchatka source region, the observations along the same Cascadia margin of the tsunami generated by the 1952 M_w 9 Kamchatka earthquake are 16 ± 10 cm. In contrast, using the full SIFT/SIM detailed inundation forecast for 20 Cascadia coastal harbors from the M_w 9.25 Aleutian event modeled by Butler et al. (2014, 2017), the maximum forecast tsunami amplitudes in harbors have a median of 166 cm and a maximum of 287 cm in Oregon.

4.6 South and Western Pacific

In the South Pacific published archeological evidence on Aitutaki in the Cook Islands and Rurutu in the Austral Islands has been interpreted by Goff et al. (2011) as long-term site abandonment due to a tsunami. Archeological excavations on Aitutaki (Allen and Wallace 2007) and Rurutu in the Austral Islands Bollt (2008) both exhibit white beach sand fining inland separating distinct ^{14}C -dated archeological occupation layers. The dates for the possible paleotsunami deposits are ca. sixteenth century AD at Aitutaki (although not securely dated) and 1450–1600 AD at Rurutu. The tsunami coastal inundation estimate for nearby Rarotonga from the modeled Aleutian event is 3 m. Nonetheless, both Allen and Wallace (2007) and Bollt (2008), respectively, proposed possible cyclone origins for the layers.

There are no extant paleotsunami deposits known to the authors from the Western Pacific subduction zones of New Britain and the Solomon Islands that have dates in the proximity of 1586 (NCEI 2017). However, the tsunami propagation from these subduction zones is dominantly blocked by islands to the north, impeding paths toward Japan.

4.7 Mexico and Central America

There are no extant paleotsunami deposits known to the authors from the Pacific coast of Mexico and Central America that have dates in the proximity of 1586 (NCEI 2017). Further, the strike of the coastal margin dominantly directs tsunami energy southwest toward the Antarctic-Pacific south of New Zealand.

5 Summary discussion

The high precision of the Kaua'i coral dates significantly improves our understanding of the tsunami that inundated the Makauwahi sinkhole. A known "orphan" tsunami in 1585/1586 in Japan fits within the uncertainty of the coral dates (1572 ± 21) and matches the forecast amplitude based upon the Eastern Aleutian earthquake model of Butler et al. (2014) within the uncertainty present. Reviewing available evidence around the Pacific, we submit that the Aleutian margin, and not Peru, is the leading candidate for the origin of the orphan Sanriku tsunami of 1586.

The Eastern Aleutian Islands are the most probable source region for the major marine incursion on Kaua'i at Makauwahi sinkhole (Butler et al. 2014) from a M_w 9.25 earthquake. With rupture from the east to west into the zone of the 1957 earthquake, such an event may produce sufficient coastal run-ups, coupled with favorable tides, to be observed in Sanriku. We also propose that a paleotsunami deposit near Sendai, Japan (Sawai et al. 2008), previously unexplained by local earthquakes may also be due to the 1586 orphan tsunami.

Ninomiya (1960), Solov'ev and Go (1975), and Iida (1984) have ascribed this orphan tsunami to an earthquake in Peru, yet earlier authors attribute the Peruvian earthquake and Sanriku tsunami as separate events (e.g., Mallet and Mallet 1858). Regarding the provenance of the 1586 Sanriku tsunami, Okal et al. (2006) have noted inconsistencies with a Peruvian source region. Iseismal intensities of the 1586 earthquake compare favorably with recent, proximal Peruvian earthquakes in 1974 and 2007. Tsunami amplitude observations and forecasts in Sanriku from these latter earthquakes are insufficient to be consistent with the 1586 Sanriku tsunami.

We have conducted a literature survey of available paleotsunami data around the Pacific, reviewing other candidate locations for the source of the 1586 tsunami in Fig. 5. The South American Pacific coast offers no other paleo-observations or historical accounts. However, there are also no historical accounts in South America of the tsunami from 1737 great Kamchatka earthquake, considered to be larger than M_w 9 Kamchatka earthquake of 1952 (Pinegina and Bourgeois 2001), though the latter event registered more than a meter at several locations in Chile.

The Cascadia margin along the Pacific northwest shows paleotsunami evidence for an event between the great 1700 earthquake and tsunami (Atwater et al. 2005) and a prior Cascadia event constrained by turbidite dating to be earlier than 1586. Considering Kamchatka as a possible source region for a 1586 tsunami, we note that the 1952 M_w 9 earthquake produced tsunami amplitudes averaging 16 cm along the Pacific Northwest coast, whereas tsunami model forecasts of an Eastern Aleutian earthquake give median tsunami coastal estimates of nearly 3 m with a maximum of 9 m. These observations and forecasts favor an Eastern Aleutian tsunami source region.

Paleotsunami and archeological data in the region of the M_w 9.2 Alaska earthquake of 1964 indicate a tsunami event at Kodiak occurring (1440–1620 A.D.) within the precision of the Kaua'i coral dates. This event could be due to an earthquake of $8 < M_w < 9$ at Kodiak Island or from an Eastern Aleutian event. Given the fault geometry and smaller size of the possible Kodiak earthquake, this is an unlikely source for the 1586 tsunami—in the context of 38 ± 26 cm observations in Sanriku from the huge Alaska 1964 event. However, an Eastern Aleutian tsunami source region may be consistent with the paleo-observations.

The first published ^{14}C -dated paleotsunami evidence (Witter et al. 2015) in the easternmost Aleutians neither confirms nor contradicts our hypothesis, and further fieldwork is planned. Two archeological sites in the Cook and Austral Islands of the South Pacific have a less certain origin, but encompass the date range of the Kaua'i coral samples.

As noted in Butler et al. (2014) the provenance of the Kaua'i tsunami deposit at Makauwahi is not yet certain, whether due to a tele-tsunami from the Aleutians or from a large local landslide. Nonetheless, we have observed 4 M_w 9.0 + earthquakes in the Pacific in 111 years, and having several such events in the sixteenth century cannot be considered unlikely. Although there is evidence for local mega-tsunamis caused by giant submarine landslides due to flank collapse of the volcanic edifices making up the Hawaiian Islands, the youngest of these events is $> 10,000$ yrs BP (McMurtry et al. 2004). Of the more recent Holocene record, apart from depositional evidence from recent large tsunamis (e.g., 1946, 1957) there is scant evidence in the literature. This uncertainty is being resolved in further paleotsunami investigations both in the Aleutians and in Hawai'i.

Finally, we would welcome the interest of Japanese colleagues in resolving the date of the 1586 tsunami through review of additional documents available in Japan not accessible by ourselves. It would also be beneficial to model an Aleutian tsunamigenic earthquake jointly for the tsunami forecasts at Makauwahi Cave sinkhole on Kaua'i and the Sanriku coast of Japan. Such a study would use detailed DEMs and bathymetry along the Sanriku coast, considering possible variations in rupture velocity, fault slip, and rupture area—extending from the Eastern Aleutians into the zone of the 1957 earthquake in the Central Aleutian Islands.

Acknowledgements We thank Denys von der Haar for assistance with the Th-U analytical chemistry and L. Neil Frazer for discussions of Bayesian methods. Kenji Satake provided helpful comments in his review. HIGP Contribution Number 2254 and SOEST Contribution Number 9994.

Data statement We are following NSF-GEO guidelines for sample and laboratory-based analytical data. Samples and sample metadata have been registered with SESAR (geosamples.org) and will be made publicly available upon publication of the paper. Coral U-series measured and derived data will be made available through the Geochron national archive managed by IEDA (Integrated Earth Data Alliance) and assigned a dataset DOI upon publication of the paper. Geochron is the preferred archive for geochronology data but is currently being adapted to host our data (it only supports U–Pb and Ar–Ar at present). Rubin is currently funded by NSF with several others to extend the Geochron archive to include U-series age data, so this capability will be available by the end of calendar year 2017.

References

- Acosta J (1621) *Histoire naturelle et morale des Indes, tant Orientais, qu'Occidentals etc*, Paris, pp 125–126
- Allen MS, Wallace R (2007) New evidence from the east Polynesian gateway: substantive and methodological results from Aitutaki, southern Cook Islands. *Radiocarbon* 49:1163–1179

- Askew BL, Algermissen ST (1985). Catalog of Earthquakes for South America, Hypocenter and Intensity Data, vol 5—Chile. Centro Regional de Sismología para America del Sur, Lima, Peru
- Atwater BF, Musumi-Rokkaku S, Satake K, Tsuji Y, Ueda K, Yamaguchi DK (2005) The orphan tsunami of 1700. Univ. of Wash. Press, Seattle
- Beauval C, Hugo Y, Bakun WH, Egred J, Alvarado A, Singaicho J-C (2010) Locations and magnitudes of historical earthquakes in the Sierra of Ecuador (1587–1996). *Geophys J Int* 181(3):1613–1633
- Bollt R (2008) Excavations in Peva Valley, Rurutu, Austral Islands (East Polynesia). *Asian Perspect* 47:156–187
- Briggs GG, Peterson CD (1992) Neotectonics of the south-central Oregon coast as recorded by late Holocene paleosubidence of marsh systems. *Geol Soc Am Abstr Programs* 24:9–10
- Bronk-Ramsey C (2009) Bayesian analysis of radiocarbon dates. *Radiocarbon* 51:337–360
- Burney DA (2002) Late Quaternary chronology and stratigraphy of twelve sites on Kaua'i. *Radiocarbon* 44(1):13–44
- Burney DA, Kikuchi WKP (2006) A millennium of human activity at Makauwahi Cave, Maha'ulepu, Kaua'i. *Hum Ecol* 34:219–247. doi:[10.1007/s10745-006-9015-3](https://doi.org/10.1007/s10745-006-9015-3)
- Burney DA, James HF, Burney LP, Olson SL, Kikuchi W, Wagner WL, Burney M, McCloskey D, Kikuchi D, Grady FV, Gage R, Nishek R (2001) Fossil evidence for a diverse biota from Kaua'i and its transformation since human arrival. *Ecol Monogr* 71(4):615–641
- Butler R, Burney DA, Walsh D (2014) Paleotsunami evidence on Kaua'i and numerical modeling of a great Aleutian tsunami. *Geophys Res Lett* 41(19):6795–6802. doi:[10.1002/2014GL061232](https://doi.org/10.1002/2014GL061232)
- Butler R, Frazer LN, Templeton WJ (2016) Bayesian probabilities for Mw 9.0+ earthquakes in the Aleutian Islands from a regionally scaled global rate. *J Geophys Res Solid Earth* 121(B5):3586–3608. doi:[10.1002/2016JB012861](https://doi.org/10.1002/2016JB012861)
- Butler R, Walsh D, Richards K (2017) Extreme tsunami inundation in Hawai'i from Aleutian-Alaska subduction zone earthquakes. *Nat Hazards* 85(3):1591–1619. doi:[10.1007/s11069-016-2650-0](https://doi.org/10.1007/s11069-016-2650-0)
- Carver G, Plafker G (2008) Paleoseismicity and neotectonics of the Aleutian subduction zone—an overview. In: Freymueller JT, Haeussler PJ, Wesson R, Ekström G (eds) Active tectonics and seismic potential of Alaska. American Geophysical Union Monograph, vol 179, pp 43–64
- Cisternas M, Atwater BF, Torrejón F, Sawai Y, Machuca G, Lagos M, Eipert A, Youlton C, Salgado I, Kamataki T, Shishikura M, Rajendran CP, Malik JK, Rizal Y, Husni M (2005) Predecessors of the giant 1960 Chile earthquake. *Nature* 437(7057):404–407
- Cobb KM, Charles CD, Cheng H, Kastner M, Edwards RL (2003) U/Th-dating living and young fossil corals from the central tropical Pacific. *Earth Planet Sci Lett* 210:91–103
- Combellick RA (1991) Paleoseismicity of the Cook Inlet region, Alaska: evidence from peat stratigraphy in Turnagain and Knik Arms. Short Notes on Alaskan Geology 1993. State of Alaska, Department of Natural Resources, Division of Geological and Geophysical Surveys, Professional Report No. 112
- Combellick RA (1993) The penultimate great earthquake in south-central Alaska: evidence from a buried forest near Girdwood. Short Notes on Alaskan Geology 1993. State of Alaska, Department of Natural Resources, Division of Geological and Geophysical Surveys, Professional Report No. 113, pp 7–15
- Combellick RA (1994) Investigation of peat stratigraphy in tidal marshes along Cook Inlet, Alaska, to determine the frequency of 1964-style great earthquakes in the Anchorage region. Report of Investigations 94-7. State of Alaska, Department of Natural Resources, Division of Geological and Geophysical Surveys
- Combellick RA, Reger RD (1994) Sedimentological and radiocarbon-age data for tidal marshes along eastern and upper Cook Inlet, Alaska. State of Alaska, Department of Natural Resources, Division of Geological and Geophysical Surveys, Report of Investigations 94-6
- Dariento ME (1991) Late Holocene paleoseismicity along the northern Oregon coast. Ph.D. dissertation, Portland State University
- Dariento ME, Peterson CD (1995) Magnitude and frequency of subduction zone earthquakes along the northern Oregon coast in the past 3000 years. *Or Geol* 57:3–12
- Dorbath L, Cisternas A, Dorbath C (1990) Assessment of the size of large and great historical earthquakes in Peru. *Bull Seismol Soc Am* 80(3):551–576
- Dura T, Cisternas M, Horton BP, Ely LL, Nelson AR, Wesson RL, Pilarczyk JE (2015) Coastal evidence for Holocene subduction-zone earthquakes and tsunamis in central Chile. *Quat Sci Rev* 113:93–111
- Easton WH, Olson EA (1976) Radiocarbon profile of Hanauma Reef, Oahu, Hawai'i. *Geol Soc Am Bull* 87:711–719
- Edwards RL, Taylor FW, Wasserburg GJ (1988) Dating earthquakes with high-precision thorium-230 ages of very young corals. *Earth Planet Sci Lett* 90:371–381
- Edwards RL, Gallup CD, Cheng H (2003) Uranium-series dating of marine and lacustrine carbonates (in Uranium-series geochemistry). *Rev Mineral Geochem* 52:363–405

- Ford MR (2014) The application of PIT tags to measure transport of detrital coral fragments on a fringing reef: Majuro Atoll, Marshall Islands. *Coral Reefs* 33:375–379. doi:[10.1007/s00338-014-1131-8](https://doi.org/10.1007/s00338-014-1131-8)
- Ford MR, Kench PS (2012) The durability of bioclastic sediments and implications for coral reef deposit formation. *Sedimentology* 59:830–842. doi:[10.1111/j.1365-3091.2011.01281.x](https://doi.org/10.1111/j.1365-3091.2011.01281.x)
- Gica E, Spillane MC, Titov VV, Chamberlin CD, Newman JC (2008) Development of the forecast propagation database for NOAA's short-term inundation forecast for tsunamis (SIFT). NOAA Technical Memorandum OAR PMEL-139, Pacific Marine Environmental Laboratory, Seattle, WA
- Gilpin LM (1995) Holocene paleoseismicity and coastal tectonics of the Kodiak Islands, Alaska, Doctoral Dissertation, University of California, Santa Cruz
- Goff J, Chague-Goff C, Dominey-Howes D, McAdoo BG, Cronin S, Bonte-Grapetin M, Nichol S, Horrocks M, Cisternas M, Lamarche G, Pelletier B, Jaffe B, Dudley W (2011) Paleotsunamis in the Pacific Islands. *Earth-Sci Rev* 107:141–146
- Goldfinger C, Nelson CH, Johnson JE, Morey AE, Gutiérrez-Pastor J, Karabanov E, Eriksson AT, Gràcia E, Dunhill G, Patton J et al (2012). Turbidite event history: methods and implications for Holocene paleoseismicity of the Cascadia Subduction Zone. U.S. Geological Survey Professional Paper 1661-F
- Hamilton S, Shennan I (2005a) Late Holocene relative sea-level changes and the earthquake deformation cycle around upper Cook Inlet, Alaska. *Quat Sci Rev* 24(12–13):1479–1498
- Hamilton S, Shennan I (2005b) Late Holocene great earthquakes and relative sea-level change at Kenai, southern Alaska. *J Quat Sci* 20(2):95–111
- Hatori T (2005) Distribution of cumulative tsunami energy from Alaska-Aleutians to western Canada. In: Satake K (ed) *Tsunamis: case studies and recent developments*. Springer, Netherlands, pp 193–201
- Hay J (1605) *De Rebus Japonicis, Indicis & Peruanis Epistolae Recentiores*. J. Hay, ed., Antwerp
- Heck NH (1947) List of seismic sea waves. *Bull Seismol Soc Am* 37(4):269–286
- Hutchinson I, Crowell AL (2006). Great earthquakes and tsunamis at the Alaska subduction zone: geoarchaeological evidence of recurrence and extent. NEHRP Grant 01-HQ-GR-0022 final report. United States Geological Survey
- Hutchinson I, Crowell AL (2007) Recurrence and extent of great earthquakes in southern Alaska during the late Holocene from an analysis of the radiocarbon record of land-level change and village abandonment. *Radiocarbon* 49(3):1323–1385
- Hutchinson I, Guilbault JP, Clague JJ, Bobrowsky PT (2000) Tsunamis and tectonic deformation at the northern Cascadia margin: a 3000-year record from Deserted Lake, Vancouver Island, British Columbia, Canada. *Holocene* 10(4):429–439
- Iida K (1984) Catalog of tsunamis in Japan and its neighboring countries. Aichi Institute of Technology, Yachigusa, Yakusa-cho, Toyota-shi, 470-03, Japan
- Iida K, Cox DC, Pararas-Carayannis G (1967) Preliminary catalogue of tsunamis occurring in the Pacific Ocean. Hawaii Institute of Geophysics, University of Hawaii, No. HIG-67-10
- Kämpfer E (1727) *History of Japan*, London
- Krashennnikov SP (1755) Description of the Kamchatka Land. St. Petersburg., in Russian; English translations since 1764
- Liebherr JK, Porch N (2015) Reassembling a lost lowland carabid beetle assemblage (*Coleoptera*) from Kauai, Hawaiian Islands. *Invertebr Syst* 29:191–213. doi:[10.1071/IS14047](https://doi.org/10.1071/IS14047)
- Lomnitz C (1970) Major earthquakes and tsunamis in Chile during the period 1535 to 1955. *Geol Rundsch* 59:938–960. doi:[10.1007/BF02042278](https://doi.org/10.1007/BF02042278)
- Mallet R (1855) Third report of the facts of earthquake phenomena. Catalogue of recorded earthquakes from 1606 B.C. to A.D. 1850 (1606 B.C.–1755). Rept. 24th Meet. British Association for the Advancement of Science, London
- Mallet R, Mallet JW (1858) The Earthquake Catalogue of the British Association with the Discussion, Curves, and Maps Etc. From the Transactions of the British Association for the Advancement of Science, 1852–1858, Being Third and Fourth Reports: London, Taylor & Francis, Red Lion Court, Fleet Street
- McMurtry GM, Watts P, Fryer G, Smith JR, Imamura F (2004) Giant landslides, mega-tsunamis, and paleo-sea level in the Hawaiian Islands. *Mar Geol* 203:219–233
- Moernaut J, Van Daele M, Heirman K, Fontijn K, Strasser K, Pino M, Urrutia R, De Batist M (2014) Lacustrine turbidites as a tool for quantitative earthquake reconstruction: new evidence for a variable rupture mode in south-central Chile. *J Geophys Res*. doi:[10.1002/2013JB010738](https://doi.org/10.1002/2013JB010738)
- Mori N, Takahashi T, Yasuda T, Yanagisawa H (2011) Survey of 2011 Tohoku earthquake tsunami inundation and run-up. *Geophys Res Lett* 38:L00G14. doi:[10.1029/2011GL049210](https://doi.org/10.1029/2011GL049210)
- National Centers for Environmental Information (NCEI). *Tsunami Database*. <https://www.ngdc.noaa.gov/ndbc/struts/form?t=101650&s=7&d=7>. Accessed April 2017

- Ninomiya S (1960) Tsunami in Tohoku coast induced by earthquake in Chile; a chronological review. *Tohoku Kenkyu* 10:19–23 (in Japanese with English summary)
- Okal EA, Borrero JC, Synolakis CE (2006) Evaluation of tsunami risk from regional earthquakes at Pisco, Peru. *Bull Seismol Soc Am* 96(5):1634–1648
- Parish W (1836) XXXIII. On the effects of the earthquake waves on the coasts of the Pacific. *Lond Edinb Philos Mag J Sci* 8(46):181–186
- Parish W (1838) Earthquake waves on the coast of the Pacific. *Proc R Geol Soc Lond* 2(N 42):214–216
- Peters R, Jaffe B, Gelfenbaum G (2007) Distribution and sedimentary characteristics of tsunami deposits along the Cascadia margin of western North America. *Sed Geol* 200:372–386
- Peterson CD, Darienzo ME (1996) Discrimination of climatic, oceanic, and tectonic mechanisms of cyclic marsh burial, Alsea Bay, Oregon. In: *Assessing earthquake hazards and reducing risk in the Pacific Northwest*. US Geological Survey Professional Paper 1560, pp 115–146
- Peterson CD, Darienzo ME, Burns SF, Burris WK (1993) Field trip guide to Cascadia paleoseismic evidence along the northern Oregon coast: evidence of subduction zone seismicity in the central Cascadia margin. *Or Geol* 55:99–114
- Pietruszka AJ, Rubin KH, Garcia MO (2001) 226 Ra–230 Th–238 U disequilibria of historical Kilauea lavas (1790–1982) and the dynamics of mantle melting within the Hawaiian plume. *Earth Planet Sci Lett* 186 (1):15–31
- Pinegina TK, Bourgeois J (2001) Historical and paleo-tsunami deposits on Kamchatka, Russia: long-term chronologies and long-distance correlations. *Nat Hazards Earth Syst Sci* 1:177–185
- Pinegina TK, Bazanova LI, Melekestsev IV, Braitseva OA, Storcheus AV, Gusiakov VK (2000) Prehistorical tsunamis on the shores of Kronotsky Bay, Kamchatka, Russia: a progress report. (in Russian), *Volcanology and Seismology*, N2, 66–74, English edition. *Volcanol Seismol* 22:213–226
- Pinegina TK, Bourgeois J, Bazanova LI, Melekestsev IV, Braitseva OA (2003) A millennial-scale record of Holocene tsunamis on the Kronotskiy Bay coast, Kamchatka, Russia. *Quat Res* 59:36–47
- Ponyavin ID (1965) Tsunami waves. *Gidrometeoizdat, Leningrad*, p 110
- Rubin KH, Fletcher CH, Sherman CE (2000) Fossiliferous Lana'i deposits formed by multiple events rather than a single giant tsunami. *Nature* 408:657–681
- Satake K, Atwater BF (2007) Long-Term Perspectives on Giant Earthquakes and Tsunamis at Subduction Zones. *Annu Rev Earth Planet Sci* 35:349–374. doi:[10.1146/annurev.earth.35.031306.140302](https://doi.org/10.1146/annurev.earth.35.031306.140302)
- Sawai Y, Fujii Y, Fujiwara O, Kamataki T, Komatsubara J, Okamura Y, Satake K, Shishikura M (2008) Marine incursions of the past 1500 years and evidence of tsunamis at Sujjin-numa, a coastal lake facing the Japan Trench. *Holocene* 18(4):517–528
- Schlichting RB (2000) Establishing the inundation distance and overtopping height of paleotsunami from the late-Holocene geologic record at open coastal wetland sites, central Cascadia margin. M.S. thesis, Portland State University
- Schlichting RB, Peterson C, Qualman D (1999) Establishing long inundation distances of prehistoric tsunami from siliciclastic and bio-geochemical tracers in open-coast, beach plain wetlands, central Cascadia margin, USA. *EOS Trans Am Geophys Union* 80:520–521
- Shennan I, Long AJ, Rutherford MM, Innes JB, Green FM, Walker KJ (1998) Tidal marsh stratigraphy, sea-level change and large earthquakes—II: submergence events during the last 3500 years at Netarts Bay, Oregon, USA. *Quat Sci Rev* 17(4):365–393
- Shennan I, Bruhn R, Plafker G (2009) Multi-segment earthquakes and tsunami potential of the Aleutian megathrust. *Quat Sci Rev* 28:7–13. doi:[10.1016/j.quascirev.2008.09.016](https://doi.org/10.1016/j.quascirev.2008.09.016)
- Shennan I, Barlow N, Carver G, Davies F, Garrett E, Hocking E (2014a) Great tsunamigenic earthquakes during the past 1000 yr on the Alaska megathrust. *Geology* 42(8):687–690. doi:[10.1130/G35797.1](https://doi.org/10.1130/G35797.1)
- Shennan I, Bruhn R, Barlow N, Good K, Hocking E (2014b) Late Holocene great earthquakes in the eastern part of the Aleutian megathrust. *Quat Sci Rev* 84:86–97. doi:[10.1016/j.quascirev.2013.11.010](https://doi.org/10.1016/j.quascirev.2013.11.010)
- Sherman CE, Fletcher CH, Rubin KH, Simmons KR, Adey WH (2014) Sea-level and reef accretion history of marine isotope stage 7 and late stage 5 based on age and facies of submerged late Pleistocene reefs, Oahu, Hawai'i. *Quat Res* 81:138–150. doi:[10.1016/j.yqres.2013.11.001](https://doi.org/10.1016/j.yqres.2013.11.001)
- Silgado E (1973) Historia de los sismos mas notables ocurridos en el Peru (1513–1970). *Geofis Panam* 2 (1):179–243 (**English translation**)
- Solov'ev SL, Go CN (1975) Catalogue of tsunamis on the eastern shore of the Pacific Ocean. (dates include 1513–1968). Academy of Sciences of the USSR, Nauka Publishing House, Moscow (Canadian Translation of Fisheries and Aquatic Sciences no. 5078, 1984, translation available from Canada Institute for Scientific and Technical Information, National Research Council, Ottawa, Ontario, Canada KIA OS2, 293 p.)
- St. Onge G, Chapron E, Mulsow S, Salas M, Viel M, Debret M, Foucher A, Mulder T, Winiarski T, Desmet M, Costa PJM, Ghaleb B, Jaouen A, Locat J (2012) Comparison of earthquake-triggered turbidites

- from the Saguenay (Eastern Canada) and Reloncavi (Chilean margin) Fjords: implications for paleoseismicity and sedimentology. *Sed Geol* 243–244:89–107. doi:[10.1016/j.sedgeo.2011.11.003](https://doi.org/10.1016/j.sedgeo.2011.11.003)
- Tavera H, Bernal I (2008) The Pisco (Peru) earthquake of 15 August 2007. *Seismol Res Lett* 79(4):510–515
- Thompson WG, Spiegelman MW, Goldstein SL, Speed RC (2003) An open-system model for the U-series age determinations of fossil corals. *Earth Planet Sci Lett* 210:365–381
- Tsuji Y (2013) Catalog of distant tsunamis reaching Japan from Chile and Peru. 津波工学研究報告. *Tsunami Eng* 30:61–68
- von Hoff KEA (1840) *Natürlichen Veränderungen der Erdoberfläche. Chronik der Erdbeben und Vulkanusbrüche. Geschichte der durch Überlieferungen nachgewiesenen, Theil 4*
- Williams HFL, Hutchinson I, Nelson AR (2005) Multiple sources for late-Holocene tsunamis at Discovery Bay, Washington State, USA. *Holocene* 15(1):60–73
- Witter RC, Carver GA, Briggs RW, Gelfenbaum G, Koehler RD, La Selle S, Bender AM, Engelhart SE, Hemphill-Haley E, Hill TD (2015) Unusually large tsunamis frequent a currently creeping part of the Aleutian megathrust. *Geophys Res Lett* 43:76–84. doi:[10.1002/2015GL066083](https://doi.org/10.1002/2015GL066083)
- Zachariasen J, Sieh K, Taylor FW, Edwards RL, Hantoro WS (1999) Submergence and uplift associated with the giant 1833 Sumatran subduction earthquake: evidence from coral microatolls. *J Geophys Res* 104:895–919